Published in final edited form as:
Am J Physiol Cell Physiol. 2008 June ; 294(6): C1371–C1377.

Bestrophin Cl^- Channels are Highly Permeable to HCO_3^-

Zhiqiang Qu[1,2] and **H. Criss Hartzell**[1]

1 *Department of Cell Biology and Center for Neurodegenerative Disease, Emory University School of Medicine, Atlanta, GA 30322*

2 *Department of Physiology, Qingdao University School of Medicine, Qingdao, Shandong 266071, China*

SUMMARY

Bestrophin-1 (Best1) is a Cl^- channel that is linked to various retinopathies in both humans and dogs. Dysfunction of the Best1 Cl^- channel has been proposed to cause retinopathy because of altered Cl^- transport across the retinal pigment epithelium (RPE). In addition to Cl^-, many Cl^- channels also transport HCO_3. Because HCO_3^- is physiologically important in pH regulation and in fluid and ion transport across the RPE, we measured the permeability and conductance of bestrophins to HCO_3^-relative to Cl^-. Four human bestrophin homologues (hBest1, hBest2, hBest3 and hBest4) and mouse Best2 (mBest2) were expressed in HEK cells and the relative HCO_3^- permeability (P_{HCO3}/P_{Cl}) and conductance (G_{HCO3}/G_{Cl}) were determined. P_{HCO3}/P_{Cl}^- was calculated from the change in reversal potential (E_{rev}) produced by replacing extracellular Cl^- with HCO_3^-. hBest1 was highly permeable to HCO_3^- (P_{HCO3}/P_{Cl}^- = ~0.44). hBest2, hBest4 and mBest2 had an even higher relative HCO_3^-permeability (P_{HCO3}/P_{Cl}^- = 0.6 – 0.7). All four bestrophins had HCO_3^- conductances that were nearly the same as Cl^- (G_{HCO3}/G_{Cl}^- = 0.9 – 1.1). Extracellular Na did not affect the permeation of hBest1 to HCO_3^-. At physiological HCO_3^- concentration, HCO_3^- was also highly conductive. The hBest1 disease-causing mutations Y85H, R92C and W93C abolished both Cl^- and HCO_3^- currents equally. V78C mutation changed P_{HCO3}/P_{Cl}^- and G_{HCO3}/G_{Cl}^- of mBest2 channels. These results raise the possibility that disease-causing mutations in hBest1 produce disease by altering HCO_3^- homeostasis as well as Cl^- transport in the retina.

Keywords

Cl channel; Bestrophins; HCO3 transport; pH; retinal pigment epithelium; retinopathy

Introduction

Bestrophins are a newly-identified family of membrane proteins that exhibit Cl^- channel activity and also function as regulators of voltage-gated Ca^{2+} channels (for review, see (10)). Human bestrophin 1 (hBest1) was first identified as the gene responsible for Best vitelliform macular dystrophy (Best disease) (24;28), but Best1 mutations have subsequently been shown to be associated with several other retinopathies in humans and dogs (10). The Best1 gene product is located in the basolateral membrane of the retinal pigment epithelium (RPE) (2; 21). It has been proposed that Best1-associated retinopathies are caused by Cl^- channel dysfunction because hBest1 mutations characteristically reduce the light peak of EOG, which reflects a basolateral Cl^- conductance in the RPE (7;10), and because many disease-causing mutations alter the Cl^- channel function of hBest1 (40;46;47). However, an alternative view

Corresponding author: Zhiqiang Qu, Department of Cell Biology, Emory University School of Medicine, 615 Michael St. 535 Whitehead Building, Atlanta, GA 30322-3030 USA, zqu@emory.edu, Tel: 001-404-727-6260; Fax: 001-404-727-6256.

holds that hBest1 is not a Cl^- channel and that its ability to regulate voltage-gated Ca^{2+} channels is responsible for the disease (10;22;23;35).

HCO_3^- is an important physiological anion that is involved in several physiological processes including pH regulation (4). Transmembrane movement of HCO_3^- is mediated by specific HCO_3^- transporters in many tissues including RPE (4;7). Photoreceptors have a very high metabolic rate that produces large quantities of CO_2 and HCO_3^- (41). HCO_3^- is removed from the retina by trans-epithelial transport by the RPE (7) which is mediated at least partly by an electrogenic $Na^+/2\ HCO_3^-$cotransporter in the apical membrane of the RPE (11;15;16;18) and a Cl^-/HCO_3^-exchanger in the basolateral membrane (7).

Although many Cl^- channels are permeable to HCO_3^-, it is not known if ion channels in RPE may also participate in HCO_3^- homeostasis. Anion channels such as CFTR, ClC, CaCC and ligand-gated anion channels are permeable to HCO_3^- anions, but the HCO_3^- permeability is usually less than 25% of the Cl^- permeability (20;31;36;43). As a potential anion channel in the basolateral membrane of the RPE, hBest1 could possibly be involved in movement of HCO_3^- from inside the RPE to the choroid (30;39). In this study, we examined the permeability of bestrophins to HCO_3^- in transfected HEK293 cells. We found that bestrophins have a surprisingly high permeability and conductance to HCO_3^- anions. This conclusion suggests that disease-causing mutations in hBest1 may result in defective transport of both Cl^- and HCO_3^-. The loss of normal HCO_3^- transport by RPE may contribute to development of Best disease.

Materials and Methods

Generation of Mutations in Bestrophins and Heterologous Expression

hBest1, hBest2, hBest3 and hBest4 cDNAs in pRK5 vectors were generously provided by Jeremy Nathans (John Hopkins University). mBest2 cDNA in pCMV-SPORT6 vector was purchased from ATCC (IMAGE clone ID: 4989959). Site-specific mutations in hBest1 and mBest2 were made using a PCR-based site-directed mutagenesis kit (Quickchange; Stratagene) as described previously (30). Bestrophins or hBest1 and mBest2 mutants were cotransfected into HEK293 cells (ATCC) using FuGene-6 transfection reagent (Roche) with pEGFP (Invitrogen) to identify transfected cells. 0.1 – 1.0 μg bestrophin wild type or mutant cDNA was used to transfect one 35-mm culture dish. One day after transfection, cells were trypsinized and re-plated on glass coverslips for electrophysiological recording. Single transfected cells were used for patch clamp experiments within 3 days after transfection.

Electrophysiology

Recordings were performed using the whole-cell recording configuration of voltage patch clamp (26). Patch pipettes were made with borosilicate glass (Sutter Instrument Co.), pulled by a Sutter P-2000 puller (Sutter Instrument Co.), and fire polished. Patch pipettes had resistances of 2–3.5 MΩ (see below). The bath was grounded via a 3 M KCl^- agarose bridge connected to a $Ag/AgCl^-$ reference electrode. Changes of chamber solutions were performed by perfusing a 1-ml chamber at a speed of ~4 ml/min. The chamber was covered and 5% (for 30 mM HCO_3^- solutions) or 30% (for 140 mM HCO_3^- solutions) CO_2 in O_2 was blown between the cover and the chamber solution surface to keep the pH and P_{CO2} constant. To produce an IV curve in response to changed extracellular anions, it was important to obtain data relatively quickly before intracellular anion concentrations changed significantly. To this end, 200-ms voltage ramps from −100 to +100 mV with 10 sec start-to-start interval were used instead of voltage steps. Because the currents are time-independent, voltage ramps provide a reliable IV relationship. Holding potential was 0 mV. Data were acquired by an Axopatch 200A amplifier controlled by Clampex 8.1 via a Digidata 1322A data acquisition system (Axon

Instruments). Experiments were conducted at room temperature (22–24°C). Liquid junction potentials were calculated using Clampex 8.1 to correct E_{rev} of various ionic conditions. The standard pipette solution (high intracellular Ca solution) contained (in mM) 146 CsCl, 2 $MgCl_2$, 5 (Ca^{2+})-EGTA, 8 HEPES, 10 sucrose, pH 7.3, adjusted with NMDG. The calculated Ca^{2+} concentration in the internal solution was 4.5 μM (30). The standard extracellular solution (150 mM Cl^- solution) contained (in mM) 140 NaCl, 4 KCl, 2 $CaCl_2$, 1 $MgCl_2$, 10 glucose, 10 HEPES, pH 7.3 with NaOH. This combination of solutions set E_{rev} for Cl^- currents to zero, while cation currents carried by Na^+ or Cs^+ had very positive or negative E_{rev}, respectively. To change extracellular anions from Cl^- to HCO_3, Cl^- was replaced on an equimolar basis with HCO_3^- (140 mM HCO_3^-/10mM Cl solution). Solution osmolarity was 303–306 mOsM for both intra- and extracellular solutions (Micro Osmometer, Model 3300; Advanced Instrument). Small differences in osmolarity were adjusted by addition of sucrose or NMDG-gluconate. In some cases, extracellular Cl^- was replaced on an equiosmolar basis with SO_4 (100mM Na_2SO4, 1mM $CaCl_2$, 10 mM HEPES, pH 7.3), which is relatively impermeant through bestrophin Cl^- channels, to verify that the current was carried by Cl^- or HCO_3^-. To maintain pH, 140mM HCO_3^- solutions were bubbled with 30% CO_2 and 30 mM HCO_3^- solutions were bubbled with 5% CO_2. In addition, both solutions contained 10 mM HEPES which also helped maintain the pH to some degree. Because it is difficult to maintain pH of HCO_3^- buffered solutions, we monitored the pH at the level of the bath and found that pH was maintained in the range of pH 7.3 to 7.5. hBest1 currents are unaffected by this variation in pH. The NMDG-HCO_3^- solution was prepared by bubbling NMDG solution with 100% CO_2 to pH 7.4.

Analysis of Data

For the calculations and graphical presentation, we used OriginPro 7.0 software (Microcal). Data analyzed with student *t* test are presented as mean ± SEM. HCO_3^- permeability relative to Cl^- (P_{HCO3}/P_{Cl^-}) was determined by measuring the shift in E_{rev} upon changing the bath solution from one containing 150 Cl^- to another containing 140 mM $HCO3^-$/10 mM Cl^- (31). The permeability ratio was estimated using the Goldman-Hodgkin-Katz equation:

$$P_{HCO3}/P_{Cl} = [Cl]_i/([HCO3])_o \exp(\Delta E_{rev} F/RT)) - [Cl]_o/[HCO3]_o,$$

where ΔE_{rev} is the difference between the reversal potential obtained with the $HCO3^-$ anion on one side of the cell and that observed with symmetrical Cl^- on both sides. F, R, and T have their normal thermodynamic meanings. $HCO3^-$ conductances relative to Cl^- (G_{HCO3}/G_{Cl} ratios) were obtained from the measurement of the slope of the IV relationship between −25 and +25 mV from E_{rev}.

Results

Bestrophins are highly permeable to HCO_3^- anions

Five bestrophins (hBest1, hBest2, hBest3, hBest4 and mBest2) which had previously been well-characterized in heterologous cell systems (30;32;33;39;40) were selected for this study (Fig.1). Except for hBest3, which exhibited tiny anion currents under the standard voltage protocol (as previously reported (29)) (Fig.1C), the other four bestrophins were highly conductive and permeable to HCO_3^- ions. The slope conductance with HCO_3^- in the bath was very similar to the conductance with Cl^- in the bath, showing that Cl^- and HCO_3^- were transported equally well by bestrophins (Fig.1 F and Fig.2B). E_{rev} was shifted to the right when 140 mM Cl^- in bath was replaced with HCO_3. This is consistent with HCO_3^- having a lower permeability than Cl, but the shift was relatively small. P_{HCO3}/P_{Cl} calculated from the shift in E_{rev} by the Goldman-Hodgkin-Katz equation was 0.44 ± 0.4 for hBest1, 0.69 ± 0.4 for hBest2, 0.65 ± 0.03 for hBest4 and 0.63 ± 0.3 for mBest2 (Fig.2A). These values are remarkably high compared to other Cl^- channels. Most Cl^- channels have P_{HCO3}/P_{Cl} ratios less than 0.25.

HEK293 cells transfected with GFP only had negligibly small Cl^- or HCO_3^- conductances (Fig.1F), indicating that Cl^- and HCO_3^-anions were conducted by transfected bestrophins.

Na does not affect hBest1 permeability to HCO_3

Although we believe that the HCO_3^- permeability is mediated by hBest1, another possibility is that hBest1 regulates some kind of electrogenic transporter, such as the slc4 Na-bicarbonate transporter family, that is responsible for the current. To determine whether the permeation of HCO_3^- was dependent on Na, we examined the HCO_3^- current in a Na-free solution consisting of NMDG-HCO_3. When the bath solution was changed to NMDG-HCO_3, the E_{rev} shifted towards the right about the same amount as with $NaHCO_3$ (Fig.3A), indicating that the presence of Na did not exert a significant effect on HCO_3^- permeation. The calculated P_{HCO3}/P_{Cl} and G_{HCO3}/G_{Cl} were statistically the same for $NaHCO_3$ and NMDG-HCO_3 (Fig.3B and C). The result supports the conclusion that hBest1 is permeable to HCO_3^- anions.

Effects of pH

There are two concerns about using HCO_3^- solutions. The first concern is maintenance of extracellular pH, because pH buffering depends on equilibration between the gaseous environment and the bathing solution. To be sure that pH was well controlled, we monitored extracellular pH at the bath and found that it was maintained within a range of pH 7.3 to 7.5. To determine whether changes in extracellular pH in this range might affect the hBest1 channel, we compared hBest1 currents recorded with HEPES buffer at pH 7.3 and TAPS buffer at pH 8.1 (Fig.4A). Within this range, the reversal potential of hBest1 current was unaffected by extracellular pH and the current amplitude was reduced only 10.6% ± 2.6% (n=5). The second concern is that upon switching from HEPES-buffered solution to HCO_3-CO_2 solution, one might expect the cytosolic solution to acidify transiently as CO_2 diffuses into the cell more rapidly than HCO_3. To minimize the change in intracellular pH, we measured P_{HCO3}/P_{Cl} and G_{HCO3}/G_{Cl} with 140 mM HCO_3/10mM HEPES solution (pH 7.8) that was not gassed with CO_2 (Fig.4B). P_{HCO3}/P_{Cl} and G_{HCO3}/G_{Cl} measured under these conditions were statistically the same as for solutions that were bubbled with CO_2 (Fig.4B). We also performed experiments with 50 mM HEPES buffer at pH 7.4 in both the internal and external solutions to better control pH. P_{HCO3}/P_{Cl} and G_{HCO3}/G_{Cl} were the same as in experiments with 10 mM HEPES (Fig.4B, C). Finally, to assess whether any uncontrolled intracellular pH change might affect hBest1 current, we compared currents recorded with HEPES-buffered internal solution at pH 7.3 with currents recorded with MES-buffered solutions at pH 6.0. Current amplitudes did not change during 5 min recording with pH_i = 6.0 and the reversal potentials were not affected (Fig.4D). These control experiments rule out possible changes in pH as contributing significantly to the outcome or interpretation of the experiments.

HCO_3^- permeability of hBest1 at physiological concentrations

The concentrations of HCO_3^- used above were non-physiological. [HCO_3] in RPE cells is about 23 mM (7). In order to observe how HCO_3^- anions permeate at physiological concentrations, we compared hBest1 currents generated in the presence of symmetrical 125 mM Cl^- to those obtained with 25 mM HCO_3^- added to the 125 mM Cl^- solution. Addition of 25 mM HCO_3^- increased the anion current amplitude at +100 mV by ~ 16% (n = 7). However, changes in reversal potential were negligible. To measure a shift in E_{rev} reliably, we compared currents in 40 mM Cl^- to those in 30 mM HCO_3/10mM Cl. Osmolarity and ionic strength were kept constant by the addition of 120 mM NMDG-gluconate. The currents in 30 mM Cl^- were smaller than in 150 mM Cl, as expected for a channel with a low Cl^- affinity (Fig.5A). The reversal potential was shifted to the right when Cl^- was replaced with HCO_3^-(Fig.5A). The calculated permeability and conductance ratios were virtually identical to the values obtained with 140 mM HCO_3^- (Fig.5B and C).

hBest1 disease-causing mutants do not conduct Cl^- or HCO_3

We hypothesized that both Cl^- and HCO_3^- may permeate hBest1 through the same pore. To test this hypothesis, we selected three disease-causing mutations (Y85H, R92C and W93C) which occur in transmembrane domain 2 and are thought to disrupt the channel pore structure (30;40). These mutations have previously been shown to be non-functional as Cl^- channels. All three mutations lost their ability to conduct both Cl^- and HCO_3^- (Fig.6). The anion conductances that remained were similar to those in cells that were transfected with GFP alone. These data provide additional evidence that hBest1 encodes the channel responsible for the HCO_3^-conductance and also shows that it is likely that Cl^- and HCO_3^- share the same conduction pathway.

V78C mutation changes the permeability of mBest2 to HCO_3

In a study of the mBest2 pore structure, we found that the V78C mutation showed the highest selectivity between anionic and cationic sulfhydryl reagents (33). For this reason, we thought that this mutation might differ from wild type in relative Cl^- and HCO_3^- permeability. We found that the mutation did alter the relative permeability and conductance of mBest2 to HCO_3^- (Fig.7). Both $G_{HCO3}/G_{Cl}^-$and P_{HCO3}/P_{Cl} for the V78C mutation were less than wild type. This is consistent with the fact that HCO_3^- has a negative charge that is distributed over two oxygen atoms. Introducing a mutation at the site that exhibits high charge selectivity may result in lower HCO_3^- permeability compared to Cl.

Discussion

Anion channels such as CFTR, ClC, CaCC and ligand-gated anion channels are permeable to HCO_3, although their permeabilities to HCO_3^- are lower than Cl^-(20;31;36;43). In this study we found that several bestrophin Cl^- channels were also permeant to the HCO_3. Interestingly, the conductance for HCO_3^- was very similar to Cl^- under a variety of conditions, suggesting that under physiological conditions, a significant amount of the hBest1 current may be carried by HCO_3.

Like bestrophin, CFTR also transports HCO_3. However, with CFTR, the mechanisms are complicated. From single channel analysis, it is clear that CFTR itself can transport HCO_3^- (20;27). Estimates of CFTR P_{HCO3}/P_{Cl}^- range from 0.1 – 0.4. The highest end of this range is slightly less than the value we have obtained for bestrophins. But, in addition to transporting HCO_3^- itself, CFTR regulates HCO_3^-secretion via electrogenic Cl/HCO_3^- exchangers of the SLC26 family (13;14;38). It appears that the bulk of HCO_3^- secretion is mediated by SLC26 transporters, because HCO_3^- transport by CFTR is very small under conditions of physiological Cl^-concentration (37;44). There are several reasons to believe that with bestrophin channels, HCO_3^- is conducted by the same pore that conducts Cl. First, the hBest1 mutations we tested affect Cl^- and HCO_3^- conductance similarly. However, it is possible that a wider sampling of mutations may reveal a dissociation of HCO_3^- and Cl^- transport. In the case of CFTR, certain mutations like G551S, affect HCO_3^-conductance without changing the Cl^- conductance significantly. Second, both $Cl^-$and HCO_3^- conductances require intracellular Ca in order for the conductance to be turned on. This suggests that the Cl^- and the HCO_3^- conductance pathways are gated in a similar manner. Also, the bestrophin currents are quite large and do not exhibit significant rectification or time dependence. These properties are incompatible with either electroneutral or electrogenic exchangers. Although the possibility exits that the HCO3 conductance in the bestrophin-transfected cells may be due to up-regulation of other anion channels or exchangers by bestrophin, we think this is unlikely given that mutations affect Cl and HCO3 conductance similarly. Single channel analysis would be useful in helping to answer this question.

Possible role of HCO_3^- in Best Disease

The mechanisms underlying Best Disease are not known and are presently controversial (10). There are two hypotheses, which may not be mutually exclusive. One hypothesis is that hBest1 is a Cl^- channel and that dysfunction of the Cl^- channel disrupts the interaction between photoreceptors and retinal pigment epithelium somehow resulting in the accumulation of lipofuscin in the subretinal space and RPE cells (8;39;46;47). The other hypothesis is that hBest1 is a regulator of voltage-gated Ca channels (22;23;35). Our finding that hBest1 is highly permeable to HCO_3^- adds another dimension to the problem. If hBest1 is also capable of transporting HCO_3, it is possible that abnormal HCO_3^- transport contributes to the disease (9).

HCO_3^- is an important anion in retinal physiology. Retina is one of the most metabolically active tissue in the body and produces large amounts of CO_2 (41;42). Because photoreceptor function is inhibited by low pH (17), it is essential that CO_2 be removed from the subretinal space. The mechanisms by which pH is controlled in the retina are incompletely understood. Several HCO_3^- transport pathways have been shown to exist in the RPE (11;12;15). HCO_3^- is moved from the subretinal space into the RPE cells by an apical Na-dependent HCO_3^- transporter (7). Because the Na-bicarbonate transporter NBC1 (SLCA4) has been localized to the apical membrane of the RPE (3), NBC1 is one candidate for the apical transporter. HCO_3^- leaves the RPE into the choriocapillaris by a Cl/HCO_3^- exchanger whose molecular identity remains unknown. This basolateral transporter could possibly be a member of the SLC4 or SLC26 families (1;25;34). There is physiological evidence supporting both electroneutral and electrogenic exchange (5;6;12;19) and different species may use different transporters. The concentration of HCO_3^- in the choriocapillaris is maintained at a low level because a functional complex of carbonic anhydrase 4 and NBC1 in the choriocapillaris ensures transport of HCO_3^- into the blood. Recently, it has been found that mutations in carbonic anhydrase 4 impairs pH regulation and causes retinal photoreceptor degeneration (45). Although carbonic anhydrase 4 is expressed in the choriocapillaris, this result emphasizes the importance of removal of HCO_3^- and CO_2 from the retina.

The question arises whether the basolateral efflux of HCO_3^- may also occur through anion channels. One advantage of exchangers is that they can harness the downhill electrochemical movement of one ion to drive the uphill movement of another. The intracellular concentration of HCO_3^- in RPE cells has been estimated to be 17 – 23 mM (7;19). If the extracellular HCO_3^- concentration on the basolateral side is maintained low by HCO_3^- transport into the blood by the NBC1– carbonic anhydrase 4 complex in the choriocapillaris, the electrochemical driving force will strongly favor HCO_3^- efflux from the RPE. If this reasoning is correct, there is no need for an exchanger mechanism to drive HCO_3^- efflux. Actually, depending on the RPE membrane potential and Cl^- equilibrium potential, the Cl^- driving force could attenuate HCO_3^- efflux through a Cl/HCO_3^- exchanger rather than promoting it. Thus, a role for channel-mediated HCO_3^- efflux should be considered. Because hBest1 is localized on the basolateral membrane (21) and has a high HCO_3^-permeability, hBest1 would be a reasonable candidate for a HCO_3^- channel in this membrane. Cellular HCO_3^- plays several fundamental roles in cells: metabolism, regulation of pH, and regulation of cell volume (4). Therefore, disturbance of HCO_3^-transport in RPE by hBest1 mutations could cause Best disease by multiple mechanisms.

Acknowledgements

This study is supported by American Heart Association (Scientist Development Grant) and American Federation of Aging Research Award to ZQ and NIH grants GM60448 and EY014852 to HCH.

Reference List

1. Alper SL. Molecular physiology of SLC4 anion exchangers. Exp Physiol 2006;91:153–161. [PubMed: 16239253]
2. Bakall B, Marmorstein LY, Hoppe G, Peachey NS, Wadelius C, Marmorstein AD. Expression and localization of bestrophin during normal mouse development. Invest Ophthalmol Vis Sci 2003;44:3622–3628. [PubMed: 12882816]
3. Bok D, Schibler MJ, Pushkin A, Sassani P, Abuladze N, Naser Z, Kurtz I. Immunolocalization of electrogenic sodium-bicarbonate cotransporters pNBC1 and kNBC1 in the rat eye. AJP - Renal Physiology 2001;281:F920–F935. [PubMed: 11592950]
4. Casey JR. Why bicarbonate? Biochem Cell Biol 2006;84:930–939. [PubMed: 17215880]
5. Edelman JL, Lin H, Miller SS. Acidification stimulates chloride and fluid absorption across frog retinal pigment epithelium. Am J Physiol 1994;266:C946–C956. [PubMed: 8178967]
6. Edelman JL, Lin H, Miller SS. Potassium-induced chloride secretion across the frog retinal pigment epithelium. Am J Physiol 1994;266:C957–C966. [PubMed: 8178968]
7. Gallemore RP, Hughes BA, Miller SS. Retinal pigment epithelial transport mechanisms and their contributions to the electroretinogram. Prog Retinal Eye Res 1997;16:509–566.
8. Hartzell HC, Putzier I, Arreola J. Calcium-activated chloride channels. Annu Rev Physiol 2005;67:715–758.
9. Hartzell HC, Qu Z, Putzier I, Artinian L, Chien L-T, Cui Y. Looking chloride channels straight in the eye: bestrophins, lipofuscinosis, and retinal degeneration. Physiol 2005;20:292–302.
10. Hartzell HC, Qu Z, Yu K, Xiao Q, Chien LT. Molecular Physiology of Bestrophins: Multifunctional membrane proteins linked to Best Disease and other retinopathies. Physiol Rev. 2007in press
11. Hughes BA, Adorante JS, Miller SS, Lin H. Apical electrogenic $NaHCO_3^-$cotransport. A mechanism for HCO_3^- absorption across the retinal pigment epithelium. J Gen Physiol 1989;94:125–150. [PubMed: 2553856]
12. Kenyon E, Maminishkis A, Joseph DP, Miller SS. Apical and basolateral membrane mechanisms that regulate pHi in bovine retinal pigment epithelium. Am J Physiol 1997;273:C456–C472. [PubMed: 9277343]
13. Ko SB, Shcheynikov N, Choi JY, Luo X, Ishibashi K, Thomas PJ, Kim JY, Kim KH, Lee MG, Naruse S, Muallem S. A molecular mechanism for aberrant CFTR-dependent HCO(3)(−) transport in cystic fibrosis. EMBO J 2002;21:5662–5672. [PubMed: 12411484]
14. Ko SB, Zeng W, Dorwart MR, Luo X, Kim KH, Millen L, Goto H, Naruse S, Soyombo A, Thomas PJ, Muallem S. Gating of CFTR by the STAS domain of SLC26 transporters. Nat Cell Biol 2004;6:343–350. [PubMed: 15048129]
15. la Cour M. Rheogenic sodium-bicarbonate co-transport across the retinal membrane of the frog retinal pigment epithelium. J Physiol 1989;419:539–553. [PubMed: 2621641]
16. la CM. Kinetic properties and Na+ dependence of rheogenic Na(+)−. J Physiol 1991;439:59–72. [PubMed: 1910086]
17. Liebman PA, Mueller P, Pugh EN Jr. Protons suppress the dark current of frog retinal rods. J Physiol 1984;347:85–110. [PubMed: 6608584]
18. Lin H, Miller SS. pHi regulation in frog retinal pigment epithelium: two apical membrane mechanisms. Am J Physiol 1991;261:C132–C142. [PubMed: 1858851]
19. Lin H, Miller SS. pHi-dependent Cl-HCO_3^- exchange at the basolateral membrane of frog retinal pigment epithelium. Am J Physiol 1994;266:C935–C945. [PubMed: 8178966]
20. Linsdell P, Tabcharani JA, Rommens JM, Hou YX, Chang XB, Tsui LC, Riordan JR, Hanrahan JW. Permeability of wild-type and mutant cystic fibrosis transmembrane conductance regulator chloride channels to polyatomic anions. J Gen Physiol 1997;110:355–364. [PubMed: 9379168]
21. Marmorstein AD, Marmorstein LY, Rayborn M, Wang X, Hollyfield JG, Petrukhin K. Bestrophin, the product of the Best vitelliform macular dystrophy gene (VMD2), localizes to the basolateral membrane of the retinal pigment epithelium. Proc Natl Acad Sci USA 2000;97:12758–12763. [PubMed: 11050159]

22. Marmorstein AD, Stanton JB, Yocom J, Bakall B, Schiavone MT, Wadelius C, Marmorstein LY, Peachey NS. A model of best vitelliform macular dystrophy in rats. Invest Ophthalmol Vis Sci 2004;45:3733–3739. [PubMed: 15452084]
23. Marmorstein LY, Wu J, McLaughlin P, Yocom J, Karl MO, Neussert R, Wimmers S, Stanton JB, Gregg RG, Strauss O, Peachey NS, Marmorstein AD. The Light Peak of the Electroretinogram Is Dependent on Voltage-gated Calcium Channels and Antagonized by Bestrophin (Best-1). J Gen Physiol 2006;127:577–589. [PubMed: 16636205]
24. Marquardt A, Stohr H, Passmore LA, Kramer F, Rivera A, Weber BH. Mutations in a novel gene, VMD2, encoding a protein of unknown properties cause juvenile-onset vitelliform macular dystrophy (Best's disease). Hum Mol Genet 1998;7:1517–1525. [PubMed: 9700209]
25. Mount DB, Romero MF. The SLC26 gene family of multifunctional anion exchangers. Pflugers Arch 2004;447:710–721. [PubMed: 12759755]
26. Neher E. Ion channels for communication between and within cells. [Review] [67 refs]. Science 1992;256:498–502. [PubMed: 1373906]
27. O'Reilly CM, Winpenny JP, Argent BE, Gray MA. Cystic fibrosis transmembrane conductance regulator currents in guinea pig pancreatic duct cells: inhibition by bicarbonate ions. Gastroenterology 2000;118:1187–1196. [PubMed: 10833494]
28. Petrukhin K, Koisti MJ, Bakall B, Li W, Xie G, Marknell T, Sandgren O, Forsman K, Holmgren G, Andreasson S, Vujic M, Bergen AAB, McGarty-Dugan V, Figueroa D, Austin CP, Metzker ML, Caskey CT, Wadelius C. Identification of the gene responsible for Best macular dystrophy. Nat Genet 1998;19:241–247. [PubMed: 9662395]
29. Qu Z, Cui Y, Hartzell C. A short motif in the C-terminus of mouse bestrophin 4 inhibits its activation as a Cl^- channel. FEBS Lett 2006;580:2141–2146. [PubMed: 16563389]
30. Qu Z, Fischmeister R, Hartzell HC. Mouse bestrophin-2 is a bona fide Cl^-channel: identification of a residue important in anion binding and conduction. J Gen Physiol 2004;123:327–340. [PubMed: 15051805]
31. Qu Z, Hartzell HC. Anion permeation in Ca^{2+}-activated Cl^- channels. J Gen Physiol 2000;116:825–844. [PubMed: 11099350]
32. Qu Z, Hartzell HC. Determinants of anion permeation in the second transmembrane domain of the mouse bestrophin-2 chloride channel. J Gen Physiol 2004;124:371–382. [PubMed: 15452198]
33. Qu Z, Chien LT, Cui Y, Hartzell HC. The Anion-Selective Pore of the Bestrophins, a Family of Chloride Channels Associated with Retinal Degeneration. J Neurosci 2006;26:5411–5419. [PubMed: 16707793]
34. Romero MF, Fulton CM, Boron WF. The SLC4 family of HCO 3 - transporters. Pflugers Arch 2004;447:495–509. [PubMed: 14722772]
35. Rosenthal R, Bakall B, Kinnick T, Peachey N, Wimmers S, Wadelius C, Marmorstein A, Strauss O. Expression of bestrophin-1, the product of the VMD2 gene, modulates voltage-dependent Ca^{2+} channels in retinal pigment epithelial cells . FASEB J 2005:178–180. [PubMed: 16282372]
36. Rychkov GY, Pusch M, Roberts ML, Jentsch TJ, Bretag AH. Permeation and block of the skeletal muscle chloride channel, ClC-1, by foreign anions. J Gen Physiol 1998;111:653–665. [PubMed: 9565403]
37. Shcheynikov N, Kim KH, Kim KM, Dorwart MR, Ko SB, Goto H, Naruse S, Thomas PJ, Muallem S. Dynamic control of cystic fibrosis transmembrane conductance regulator Cl(−)/HCO3(−) selectivity by external Cl(−). J Biol Chem 2004;279:21857–21865. [PubMed: 15010471]
38. Shcheynikov N, Ko SB, Zeng W, Choi JY, Dorwart MR, Thomas PJ, Muallem S. Regulatory interaction between CFTR and the SLC26 transporters. Novartis Found Symp 2006;273:177–186. [PubMed: 17120768]
39. Sun H, Tsunenari T, Yau K-W, Nathans J. The vitelliform macular dystrophy protein defines a new family of chloride channels. Proc Natl Acad Sci USA 2002;99:4008–4013. [PubMed: 11904445]
40. Tsunenari T, Sun H, Williams J, Cahill H, Smallwood P, Yau K-W, Nathans J. Structure-function analysis of the bestrophin family of anion channels. J Biol Chem 2003;278:41114–41125. [PubMed: 12907679]
41. Wangsa-Wirawan ND, Linsenmeier RA. Retinal oxygen: fundamental and clinical aspects. Arch Ophthalmol 2003;121:547–557. [PubMed: 12695252]

42. Winkler BS. Buffer dependence of retinal glycolysis and ERG potentials. Exp Eye Res 1986;42:585–593. [PubMed: 3720873]

43. Wotring VE, Chang Y, Weiss DS. Permeability and single channel conductance of human homomeric rho1 GABAC receptors. J Physiol 1999;521 Pt 2:327–336. [PubMed: 10581305]

44. Wright AM, Gong X, Verdon B, Linsdell P, Mehta A, Riordan JR, Argent BE, Gray MA. Novel regulation of cystic fibrosis transmembrane conductance regulator (CFTR) channel gating by external chloride. J Biol Chem 2004;279:41658–41663. [PubMed: 15286085]

45. Yang Z, Alvarez BV, Chakarova C, Jiang L, Karan G, Frederick JM, Zhao Y, Sauve Y, Li X, Zrenner E, Wissinger B, Hollander AI, Katz B, Baehr W, Cremers FP, Casey JR, Bhattacharya SS, Zhang K. Mutant carbonic anhydrase 4 impairs pH regulation and causes retinal photoreceptor degeneration. Hum Mol Genet 2005;14:255–265. [PubMed: 15563508]

46. Yu K, Cui Y, Hartzell HC. The bestrophin mutation A243V, linked to adult-onset vitelliform macular dystrophy, impairs its chloride channel function. Invest Ophthalmol Vis Sci 2006;47:4956–4961. [PubMed: 17065513]

47. Yu K, Cui Y, Hartzell HC. Chloride Channel Activity of Bestrophin Mutants Associated with Mild or Late-Onset Macular Degeneration. Invest Ophthalmol Vis Sci 2007;48:4694–4705. [PubMed: 17898294]

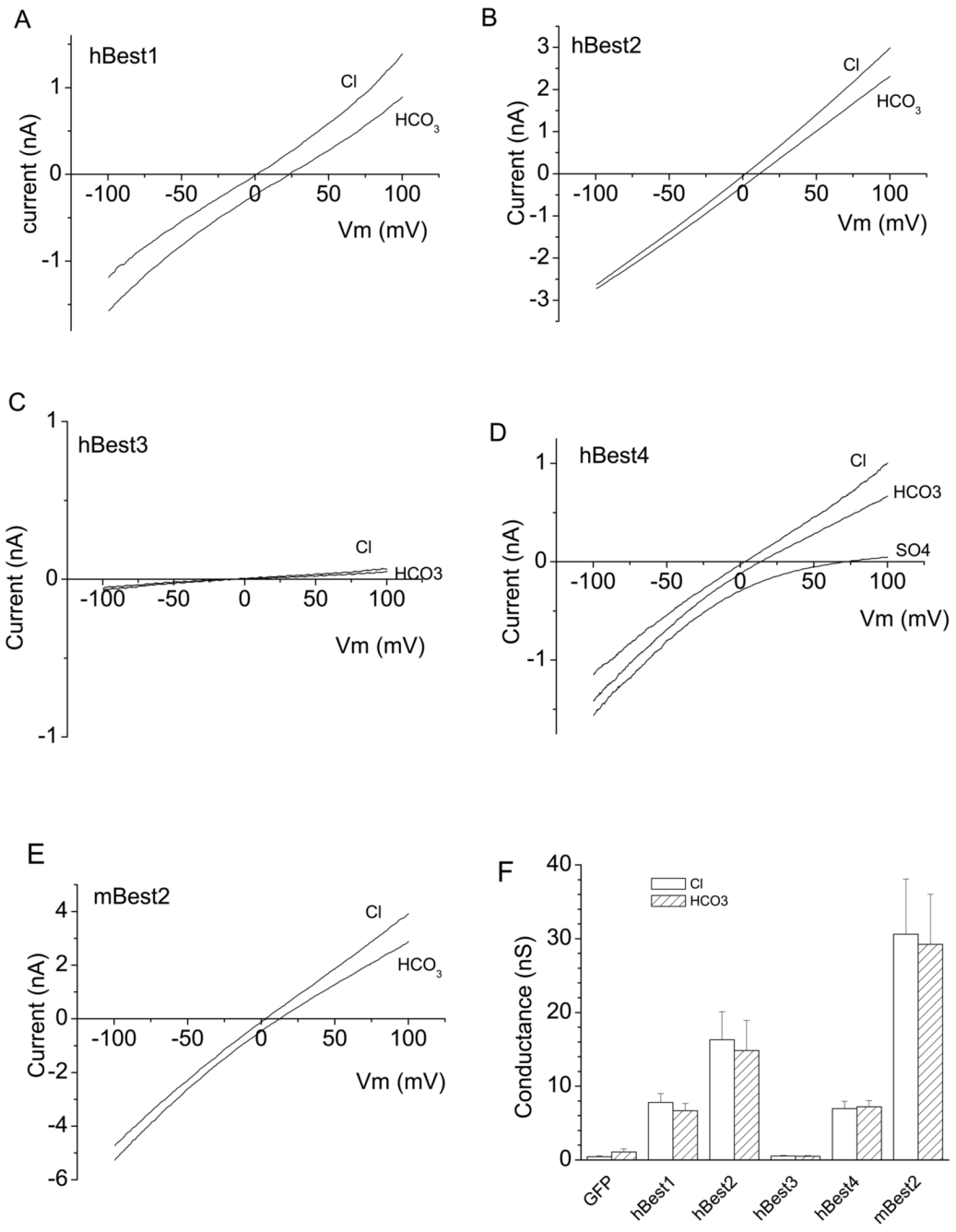

Fig.1.

Bestrophins are permeable to HCO_3. hBest1 (A), hBest2 (B), hBest3 (C), hBest4 (D) or mBest2 (E) cDNA in mammalian expression vectors were cotransfected into HEK293 cells along with GFP to identify the transfected cells. The green cells were selected for whole-cell voltage clamp recording. Cells were stimulated by ramp voltages and Cl^- currents recorded with pipette solution containing high Ca (see Methods). For measurement of bestrophin permeabilities to HCO_3^- relative to Cl, 140 mM $NaCl^-$ in bath solution was replaced with 140 $NaHCO_3^-$(see Methods), which was bubbled with 30% CO_2 to maintain pH. **A, B, C, D** and **E** are representative cells (n = 5–11). SO_4 solution was used to check the presence of leak current in

D. **F.** Average values of slope conductances of Bestrophin-expressed currents. hBest3/GFP or GFP only-transfected cells showed negligible conductance to both Cl^- and HCO_3.

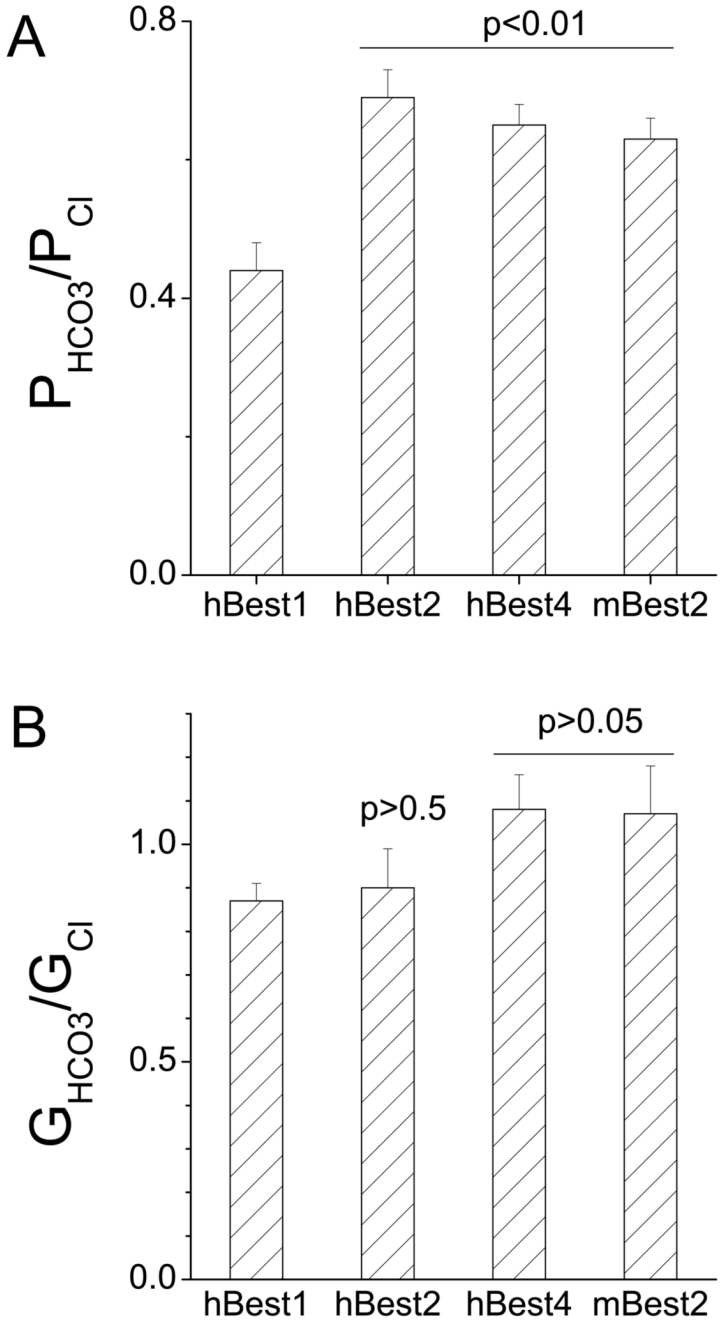

Fig.2.

Relative permeability and conductance of bestrophins to HCO_3. **A.** Relative permeabilities were determined by measuring the shift in E_{rev} produced by switching from 140 mM Cl^- to 140 mM HCO_3^- and using the Goldman-Hodgkin-Katz equation to calculate P_{HCO3}/P_{Cl}^- (see Methods). **B.** Relative conductance was measured as the slope of the I-V curve ±25 mV around the reversal potential. (n = 5–11). Statistical comparisons between hBest1 and other bestrophins are shown in A and B.

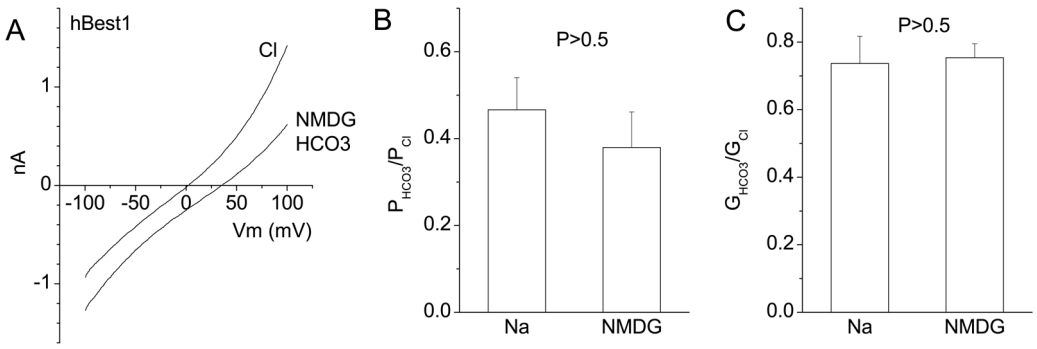

Fig.3.

Na did not affect HCO_3^- permeation across hBest1 channels. Whole-cell recordings were performed as in Fig.1 except that Na was replaced with NMDG. 140 mM NMDG-Cl^- was replaced with 140 mM NMDG-HCO_3^- (see Methods) and E_{rev} measured. **A.** Representative I-V relationships of an hBest1-expressing HEK cell bathed in NMDG-Cl^- or NMDG-HCO_3. **B** and **C.** Average relative permeabilities and conductances of hBest1 with Na or NMDG as cations. There were no significant differences between the two cations ($P > 0.5$, $n = 4–5$).

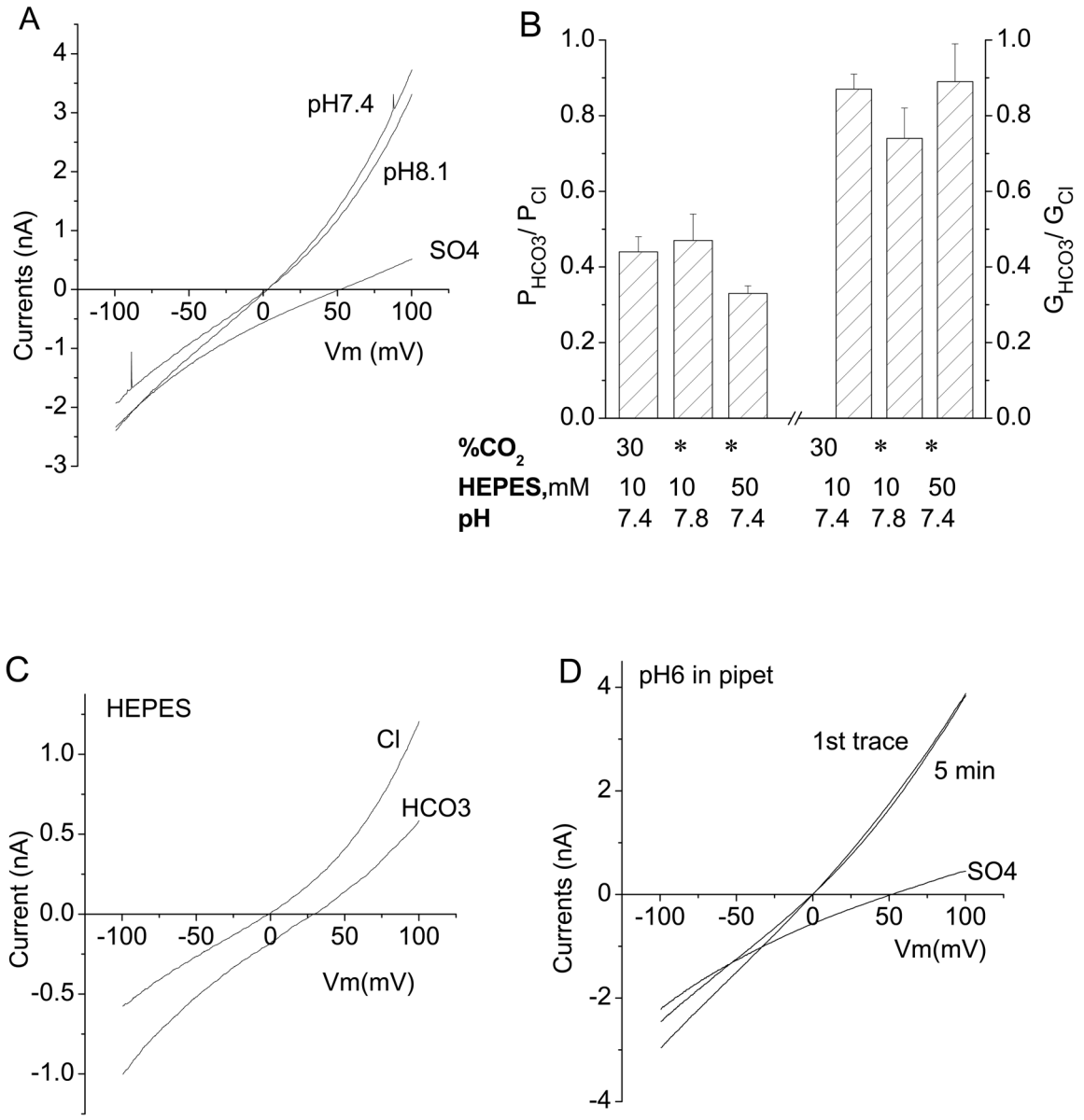

Fig.4.

Effects of pH on hBest1-expressed currents. A. Representative I-V curve from an hBest1 expressing cell bathed in normal extracellular solution (HEPES, pH 7.3) and an extracellular solution of pH 8.1 (TAPS). Raising extracellular pH from 7.3 to 8.1 had no significant effect on hBest1 currents. Replacement of extracellular Cl with SO_4 largely blocked outward currents. B. Comparison of relative permeability and conductance of HCO_3^- under various conditions as indicated. The 30% CO_2 /10 HEPES /pH 7.4 bars are the same data as in Fig.1. There are no significant differences among three groups ($P > 0.1$, $n = 5–11$). * ambient. C. Effect of buffering the solutions with 50 mM HEPES. All solutions, both internal and external, contained 50 mM HEPES. D. Representative I-V curves from hBest1 expressing cells with internal pH of 7.3 or 6.0. The pH 6.0 internal solution was buffered with MES; the pH 7.3 solution was buffered with HEPES. The result is typical of 3 cells.

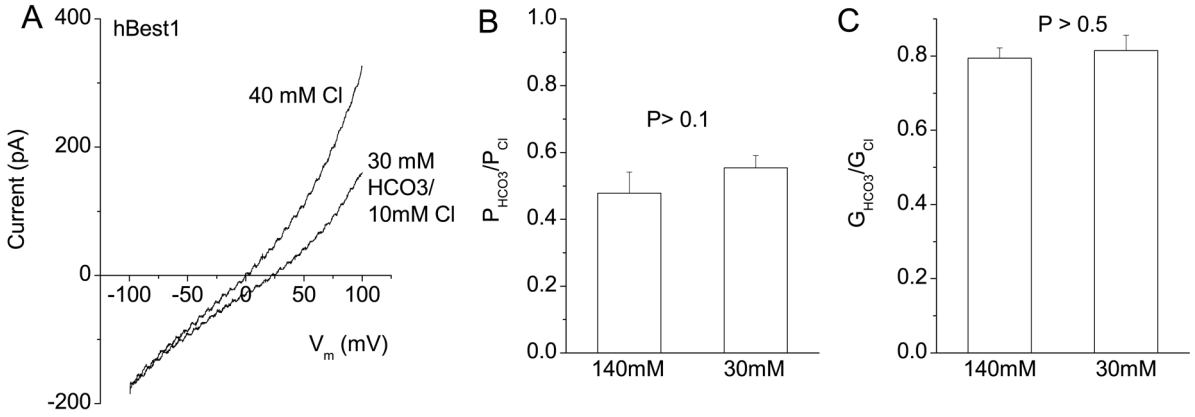

Fig.5.

Permeability of hBest1 in low HCO_3^- concentrations. Internal [Cl] was 40 mM. External solution contained 40 mM $NaCl^-$ or 30 mM $NaHCO_3^-$ solutions (with other components supplied as in 140 mM Cl^- solution, see Methods). **A.** Current traces of a representative cell recorded with low permeant anion concentrations on both sides of the cell. **B** and **C.** Relative HCO_3^- permeabilities and conductances for high (140 mM) and low (30 mM) HCO_3^- concentrations (n = 4 – 8).

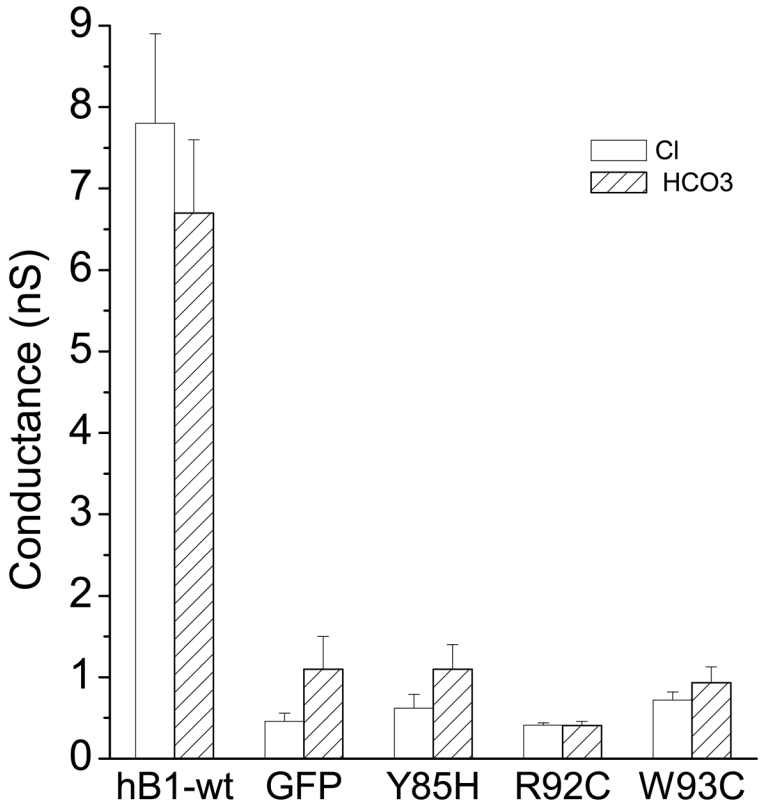

Fig.6.

Loss of both Cl^- and HCO_3^- conduction through hBest1 due to disease-causing mutations. Mutant cDNAs were transfected into HEK cells for whole-cell current recording as described in Fig.1. Average values of slope conductances were calculated as described in Methods (n = 5 – 10).

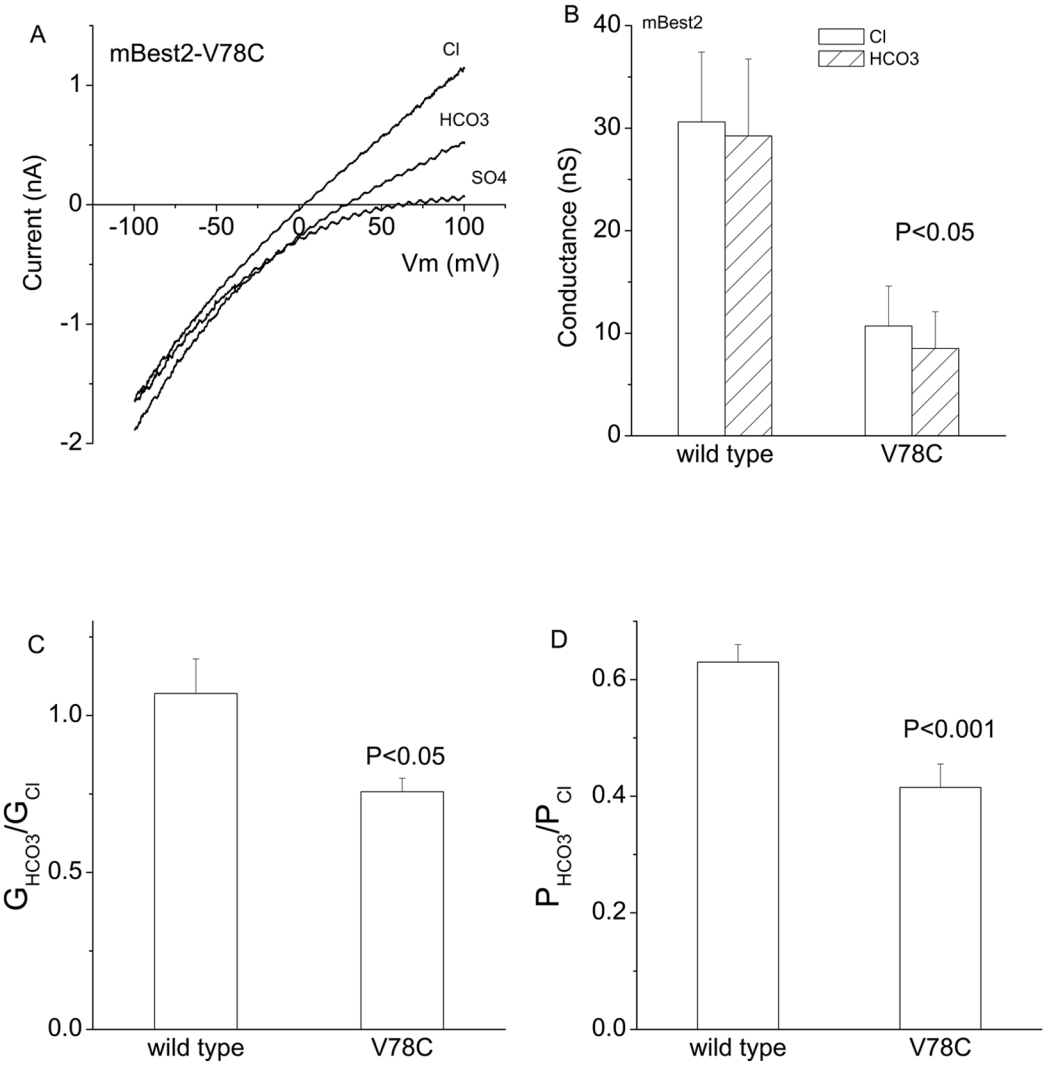

Fig.7.

V78C mutation changes the permeability of mBest2 to HCO3. As described in Fig.1, the V78C mutant cDNA was transfected into HEK cells for whole-cell current recordings. **A.** Representative current traces. **B, C** and **D.** V78C mutation significantly attenuated the slope conductances (B), relative G_{HCO3}/G_{Cl}^- (C) and P_{HCO3}/P_{Cl}^- (D), compared to mBest2 wild type (n = 5–11). Note that in B, slope conductances for both wild type and V78C between Cl^- and HCO_3^- are not significantly different (P > 0.5).